



Available online at www.sciencedirect.com

ScienceDirect

Geochimica et Cosmochimica Acta 308 (2021) 310-325

Geochimica et Cosmochimica Acta

www.elsevier.com/locate/gca

Origin of low oxygen isotopic compositions in alkalic lavas from Erebus volcano, Antarctica

Lara B. Owens a,b, Philip R. Kyle b,*, Zachary D. Sharp c, Andrew Campbell b

^a Rocky Mountain Institute, Boulder, CO 80301, USA

Received 4 January 2021; accepted in revised form 3 June 2021; Available online 9 June 2021

Abstract

Mount Erebus on Ross Island, Antarctica is an active volcano that has hosted a persistent phonolite lava lake for over 50 years. Oxygen isotope analysis of minerals in alkaline basanite to phonolite lavas from Erebus and surrounding volcanic centers show an anomalous trend of decreasing $\delta^{18}O$ with magmatic evolution. The cold frozen climate and lack of radiogenic isotope evidence for assimilation of crustal materials makes this a unique location to investigate factors contributing to changes in oxygen isotope compositions. Olivine, feldspar, glass and whole rock samples from 29 lavas, 7 modern bombs and 2 xenoliths were analyzed for their oxygen isotopic compositions. Forward models indicate there should be an enrichment in $\delta^{18}O$ of 0.4‰ in lavas due to Raleigh fractionation, but this is not observed. Olivine $\delta^{18}O$ decreases from a typical mantle value of +5.3% in the parental basanite source to 4.3‰ in recently erupted phonolite lava bombs. The trend correlates with a decreasing forsterite content in the olivine. Feldspar and glasses exhibit $\delta^{18}O$ values well below predicted values and are in fractionation disequilibrium with olivine compositions at measured magmatic temperatures of 1000 °C within the phonolite lava lake. Isotopic depletion of the melt may be accounted for by incorporation of 8–11% hydrothermally altered volcanic edifice over time assuming water–rock interaction from strongly isotopically depleted Antarctic precipitation. Enhanced disequilibrium with olivine phenocrysts, are seen during the late stages of Erebus volcano construction. This calls for differential fractionation of olivine and feldspar from their respective melts, and slow O-diffusion of olivine while in the shallow lava lake prior to eruption.

© 2021 Elsevier Ltd. All rights reserved.

Keywords: Erebus volcano; Oxygen isotopes; Antarctica; Alkaline volcanics

1. INTRODUCTION

Low δ^{18} O values (δ^{18} O < 5.5%) are widespread in silicic magmas world-wide and petrologically have been a problem to explain (Troch et al., 2020). The low δ^{18} O values are often attributed to assimilation of hydrothermally

E-mail addresses: lowens@rmi.org (L.B. Owens), philip.kyle@nmt.edu (P.R. Kyle), zsharp@unm.edu (Z.D. Sharp), andrew.campbell@nmt.edu (A. Campbell).

altered rocks or alteration by meteoric water. Alkaline magma systems, which typically evolve from alkali basalt and basanites to felsic magmas, such as phonolites and trachytes, are widespread in intraplate rift settings including many oceanic islands. Such alkaline systems evolve mainly by fractional crystallization. Oxygen isotopes can be used to trace the evolution of alkaline magmas and only rarely has evidence been reported showing evidence of low δ^{18} O values (e.g., Panter et al., 1997; Woolf et al., 2000; Harris et al., 2000). Mineral-melt fractionation factors for oxygen isotopes between magmas and typical mafic minerals involved in the fractional crystallization are negative.

^b Department of Earth and Environmental Science, New Mexico Institute of Mining and Technology, Socorro, NM 87801, USA ^c Center for Stable Isotopes, Department of Earth and Planetary Science, University of New Mexico, Albuquerque, NM 87131, USA

^{*} Corresponding author.

Therefore, magmatic evolution by fractional crystallization should result in increasing δ^{18} O in evolutionary sequences.

Erebus an active stratovolcano on Ross Island hosts a persistent convecting phonolite lava lake (Kyle, 1994; Oppenheimer and Kyle, 2008a). Petrologic and geochemical studies of the modern and historic lavas of Erebus show a well-established evolutionary history for the magmatic system (Kyle et al., 1992; Kelly et al., 2008; Sims et al., 2008, 2013; Iacovino et al., 2016; Rasmussen et al., 2017). Lava flows on Erebus volcano record two petrologic suites of lavas. The Erebus lineage (EL) has a strongly silicaundersaturated parental basanite magma which evolved

via fractional crystallization to anorthoclase-phyric phonolite with no evidence for crustal assimilation (Kyle et al., 1992; Sims et al., 2008). A contemporaneous yet volumetrically minor enriched-iron suite (EFS) of trachyandesite, phonolite and trachyte flows, evolved from a basanite parent and assimilation of crustal components is apparent in the trachytes. The Dry Valley Drilling Project (DVDP) holes 1–3 cored a lava sequence at Hut Point Peninsula (Fig. 1) (Kyle, 1981a,b). The cores and overlying lavas show a complete evolutionary suite of silica-undersaturated basanite to phonolite lavas, called the DVDP lineage. The DVDP lineage evolved by a distinct liquid line of descent

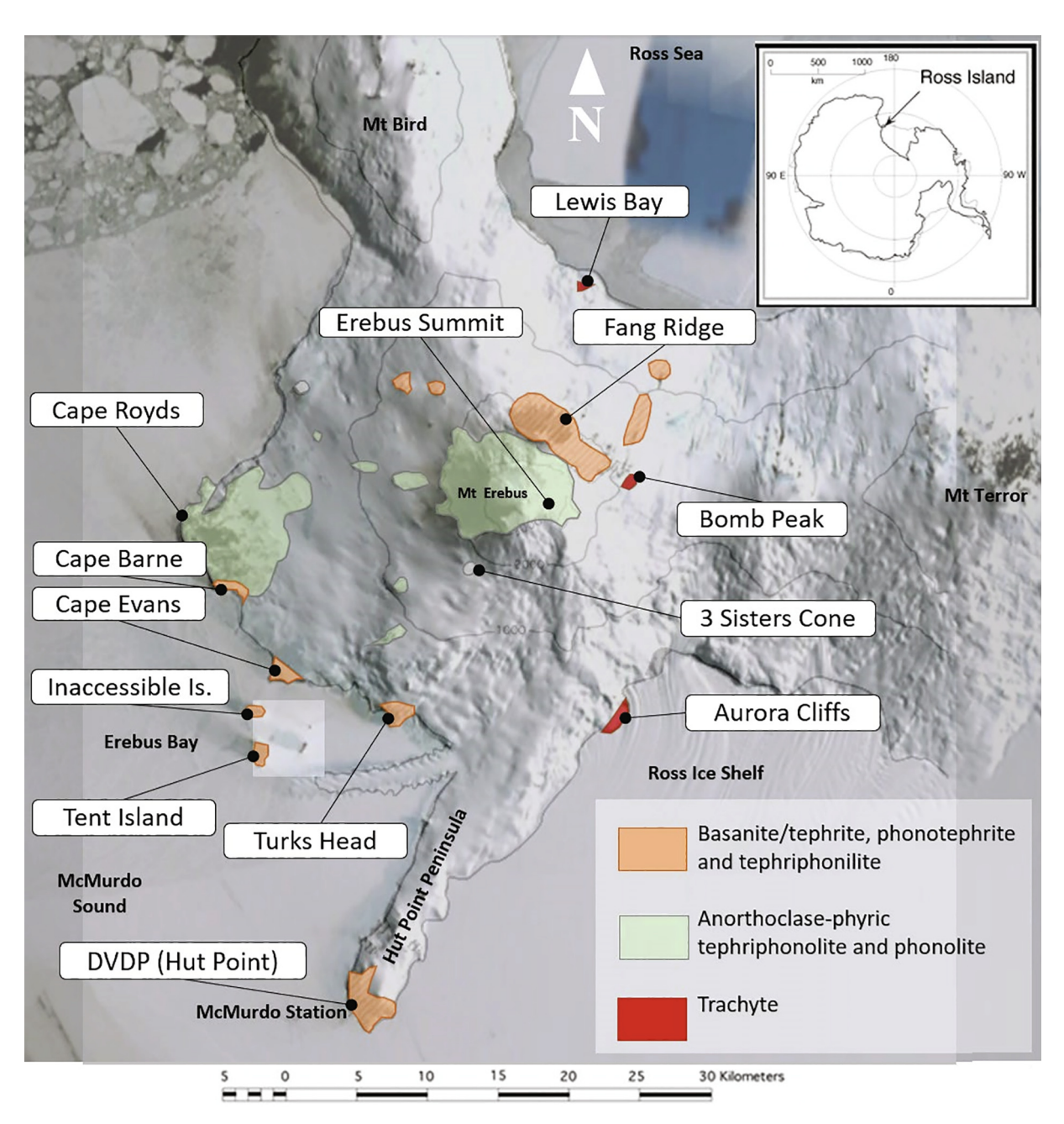


Fig. 1. Map showing locations of sample sites on Mount Erebus, islands in Erebus Bay and elsewhere on Ross Island (sample details are given in Supplemental Table S1).

compared to the EL with fractionation of olivine only in the basanites and this was replaced by the Ti-rich amphibole kaersutite in the more evolved lavas. The DVDP lineage is used here for context and comparison with the Erebus lavas. The EL, EFS and DVDP lineages are believed to have evolved from the same parental basanite best represented by the primitive MgO-rich basanites from the DVDP drill cores (Kyle et al., 1992; Iacovino et al., 2016).

In this study, we examine the oxygen isotopes in whole rock, glass, olivine and feldspar from the Erebus lineages and selected samples from the DVDP lineage to characterize temporal variations and discern the events and mechanisms responsible for observed low δ^{18} O values. This study reveals lowered oxygen isotope values in the more evolved Erebus lavas, which provides a unique opportunity to investigate alternative mechanisms for the formation of isotopically light magmas. Mineral pairs allow for temperature-dependent isotopic fractionation calculations for each stage of magmatic differentiation and qualification of crystal-melt equilibrium conditions. Whole rock oxygen isotopic data also provide comparison of overall fractionation trends between the EL, and DVDP lineages. The EFS suite is included here to compare mechanisms driving the formation of low- δ^{18} O in the evolved lavas.

2. EREBUS VOLCANO

2.1. Volcanic setting

The 3794-meter-high Erebus stratovolcano is surrounded by the 3 smaller radially distributed volcanic centers of Mounts Bird, Terror and Hut Point Peninsula (Fig. 1). Ross Island is part of the Erebus volcanic province (Kyle, 1990a) of the extensive McMurdo Volcanic Group, which occurs in the western Ross Sea area of Antarctica (Kyle, 1990b). Volcanism is associated with Cenozoic intraplate rifting within the West Antarctic Rift System (Behrendt, 1999; Jordan et al., 2020). Ross Island volcanism has been explained by a mantle plume beneath Erebus (Kyle et al., 1992; Phillips et al., 2018) but is still subject to speculation (e.g., Storey et al., 1999; Rocchi et al., 2002, 2005; Gupta et al., 2009; Panter, 2021). Each volcanic center on Ross Island has a slightly different magmatic evolutionary path, with the EL exhibiting a hotter, drier, magmatic plumbing system than the kaersutite-bearing DVDP lineage rocks found at the 3 volcanic centers (Bird. Terror and Hut Point) (Fig. 1) that radially surround Erebus (Kyle et al., 1992; Iacovino et al., 2016; Rasmussen et al., 2017).

2.2. Petrology of Erebus suites and mantle source

The EL consists of parental basanites, phonotephrite, tephriphonolite and anorthoclase-bearing tephriphonolites and phonolites (Kyle et al., 1992). Olivine, high-Al and Ti clinopyroxene, titanomagnetite, and feldspar are the main mineral phases in the fractional crystallization history of the magmas, with trace amounts of nepheline, pyrrhotite, and apatite occurring throughout. Olivine ranges from Fo₈₉ in basanites to Fo₄₇ in the anorthoclase phonolites.

Feldspar ranges from plagioclase $(An_{50}Ab_{46}Or_4)$ in less evolved samples to anorthoclase $(An_{10\text{-}23}Ab_{63\text{-}68}Or_{11\text{-}27})$ in the phonolites (Kyle et al, 1992; Kelly et al., 2008). Major and trace element compositions for EL lavas exhibit smooth fractionation trends on geochemical variation diagrams, supporting the fractional crystallization of the observed mineral phases. This scenario is supported by least-squares mass balance models for each stage of fractionation (Kyle et al., 1992) and by the uniform ratios between incompatible and compatible elements observed throughout the EL suite.

The EFS lineage lavas are rare on Erebus volcano and associated centers in Erebus Bay (Fig. 1) and consist of more silica-saturated trachyandesites, trachytes and phonolites with microphenocrysts of olivine, clinopyroxene, opaque oxides, kaersutite, and alkali to plagioclase feldspars (Kyle et al., 1992). The olivine is more iron-rich than in the EL. Incompatible elements in EFS lavas are distinct from those of EL, indicating a unique fractionation history. In EFS trachytes low Sr, Ba, and K/Rb ratios and large Eu anomalies suggest derivation from a fractionated residual magma, while elevated Pb and Sr isotopic ratios suggest some assimilation of radiogenic isotope-enriched crust (Kyle et al., 1992; Sims et al., 2008).

DVDP core samples, which define the DVDP lineage, exhibit similar mineral compositions to the EL except for the presence of kaersutite, which replacements olivine as a major phase during fractionation to form the evolutionary sequence (Kyle, 1981b; Kyle et al., 1992; Iacovino et al, 2016). The DVDP lineage formed by fractional crystallization of olivine, clinopyroxene, kaersutite, magnetite, and feldspar as shown by least-squares mass balance models (Kyle, 1981b). In the DVDP lineage major and trace elements plot linearly and similarly to EL lavas, except for decreased TiO2, FeO, and Y contents and enrichment in K and Rb in more evolved DVDP lavas due to kaersutite fractionation. Experimental studies (Iacovino et al., 2016) suggest the kaersutite-bearing DVDP lavas fractionated below 1050 °C at 200-400 MPa whereas the EL fractionation occurred above 1050 °C and pressures about 200 MPa.

Radiogenic isotopes have been used to identify the mantle source and paths of differentiation for the Erebus lavas. Near constant ⁸⁷Sr/⁸⁶Sr values, below 0.7030 throughout the Erebus lineage and DVDP lavas, argue against crustal contamination (Kyle et al., 1992; Sims et al., 2008, 2013; Phillips et al., 2018). EFS trachyte from Aurora Cliff has an elevated ⁸⁷Sr/⁸⁶Sr ratio of 0.70425 showing a definite crustal contribution to the melt. Hafnium, Nd and Pb isotopic analyses demonstrate a slightly greater degree of isotopic variation in the earliest stages of differentiation among EL and DVDP basanites and phonotephrites, which is attributed to a heterogeneous mantle source (Sims et al., 2008; Phillips et al., 2018). EL and DVDP lineage samples plot between HIMU and DMM mantle end members (Zindler and Hart, 1986). The strong HIMU signature may be associated with upwelling mantle due to rifting or a mantle plume (Kyle et al., 1992). Other authors, however, attribute this source signature to lithospheric mantle impregnated with amphibole and phlogopite (Finn et al., 2005; Panter et al., 2006; 2018). Younger phonolitic lavas (<17 ka) exhibit no variation in Sr, Hf, Nd, or Pb isotopes, indicating a stable steady-state system, an isotopically homogenous source, or very efficient magma mixing (Kelly et al., 2008; Sims et al., 2008, 2013).

2.3. Volcanic degassing

One of the most unique features of Erebus volcano is its persistent convecting phonolite lava lake with continuous degassing of H₂O, CO₂, CO, HCl, SO₂ and other minor species (Oppenheimer and Kyle, 2008b; Oppenheimer et al., 2009; 2011; Ilanko et al., 2015a, 2015b), CO₂ emission rates of 1330 Mg.d-1 have been measured and are considered to be representative of the observed 50 years of lava lake activity (Oppenheimer and Kyle, 2008a). The observed CO₂ flux, however, cannot be reconciled from a small highlevel magma reservoir alone and must be continuously streaming from a deeper (>8 kbar) CO₂-rich basanite reservoir (Wardell et al., 2004; Oppenheimer et al., 2011). Rasmussen et al., (2017) has shown clear evidence of very CO₂ rich magmas with olivine-hosted melt inclusions on Ross Island reaching 1.8 wt% CO₂. Ilanko et al., (2019) measured gas emissions in ice caves and warm geothermal ground in the summit area of Erebus and found them dominated by air and varying amounts of magmatic CO2. Carbon isotopic compositions of the CO₂ require a hydrothermal system at depth with temperatures of over 120 °C.

3. SAMPLE SELECTION AND METHODS

Thirty-six samples from the EL, EFS, and DVDP suites were analyzed for oxygen isotopes (Supplemental Table S1; Fig. 1). Anorthoclase phonolite bombs ejected by Strombolian eruptions from the phonolite lava lake at Erebus volcano were analyzed to characterize the present high-level magma system and to search for changes in oxygen isotope compositions between 1997 and 2006. Geochemical analyses of whole rock samples and glass from bombs are summarized in Table S2. High MgO (12.13 wt%) basanite sample D2-105.53 from DVDP hole 2 was used by Kyle (1981b) as a possible parental end member for the DVDP lineage and was later used as the parent for the Erebus lineage (Kyle et al., 1992) and will be used in this study for that purpose.

Whole rock and glass samples were crushed and sieved to 30 mesh and cleaned in an ultrasonic bath. Mineral separates were handpicked under a binocular microscope to select pristine olivine and feldspar samples with minimal inclusions. Whole rock/glass powders were also prepared for oxygen isotopic analysis by crushing to 250 μm and pulverizing with a Tungsten carbide swing mill. Glass was separated from the phonolite bombs erupted from Erebus to allow mineral-groundmass comparisons. Microprobe analyses were made of glass and mineral separates to provide geochemical compositions and identify zoning and alteration for each sample; this also provided quality control of the separation and preparation processes.

Oxygen isotopes were analyzed in whole rock, glass and feldspar separates at the New Mexico Tech's Stable Isotope

Lab on a traditional silicate fluorination line (Ertchi and Silverman, 1951). Samples were powdered and placed in nickel reaction vessels. Samples were reacted in an evacuated vessel with excess ClF₃ at 500 °C for eight hours to liberate O_2 from silicates. Free oxygen was converted to CO_2 by activated carbon rods and collected in liquid nitrogen traps. Lastly, CO_2 gas was analyzed with a Finnigan Delta Plus XP mass spectrometer. Analyses were calibrated to oxygen isotope standards NBS-28 quartz ($\delta^{18}O = 9.64\%$).

Oxygen isotope analyses of olivine were made by laser fluorination (Sharp, 1990) at the Stable Isotope Laboratory at the University of New Mexico. Samples were placed in an evacuated laser extraction line and heated with a 25-W Merchantek CO_2 laser in BrF_5 gas. Liberated O_2 was collected in a zeolite cold finger and analyzed in a Finnigan MAT Delta XL mass spectrometer. Analyses were calibrated using garnet standard UWG-2 ($\delta^{18}O = +5.8\%$). All data are reported in the standard notation relative to VSMOW. Raw analytical data for all samples and standards are given in Table S9.

4. RESULTS

4.1. Mineral compositions

Electron microprobe analyses of glass and mineral separates are given in Tables S3–S5. EL olivine ranges from forsterite (Fo) contents of Fo₈₉ to Fo₄₇. EFS olivines have high fayalite (Fa) contents with values of Fa₉₄ in the more evolved samples. Little to no variation was observed between mineral grains, implying a homogenous chemical composition in each stage of the melt. No xenocrystic compositions were identified. Olivine rims and cores were examined to identify evidence of resorption or late-stage growth, but no chemical zoning was observed.

In the EL suite, feldspars range in composition from $An_{50}Ab_{46}$ Or₄ in less evolved phonotephrite to $An_{10-23}Ab_{63-68}Or_{11-27}$ (Table S5) in recently erupted anorthoclase megacrysts in phonolite bombs (Kyle et al., 1992; Kelly et al., 2008). Feldspars for the EFS suite are more albiterich with typical compositions of $An_{2-4}Ab_{60-81}Or_{17-36}$.

4.2. Oxygen isotopes

Oxygen isotope analyses of 34 lava and lava bomb samples and 2 xenolith samples are given in Table 1. The whole rock lava samples and glass from phonolite bombs have δ^{18} O values with a range from 4.42 to 6.35% (Fig. 2A) with most samples having δ^{18} O values between 5.5 and 6.0%. There is some scatter in the data and there is no significant correlation with the MgO content of the sample. Phonolite glasses from recently erupted bombs have δ^{18} O ranging from 5.54 to 5.82% with an average of 5.70 \pm 0.10% (n = 5). Whole rock δ^{18} O analyses of four DVDP-2 lava core samples increase with depth from 5.48% at 45.86 m to 5.49‰ at 61.23 m, 5.66‰ at 76.38 m and 6.02‰ at 105.53 m (Table 1). The δ^{18} O decreases slightly and systematically with decreasing MgO contents (Fig. 2A). A cumulate xenolith (82431) has low δ^{18} O values for olivine, feldspar, and whole-rock samples of -2.1, -0.2 and

Table 1
Oxygen isotope analyses of whole rock/glass, olivine, and feldspar from Erebus volcano and DVDP core samples.

Sample	Location	Rock Type	MgO (wt%)	WR/glass		Olivine*			Feldspar			Δ^{18} O(a-b)					
				δ18Ο (‰)	n/SD	Fo%	δ18Ο (‰)	n/SD	An%	δ ¹⁸ O (‰)	n/SD	(Ol-Fsp)	T °C	(Fsp-WR)	T °C	(Ol-WR)	T °C
DVDP LIN	IEAGE																
D3-295.43	DVDP 3	Bas	13.78			85.1	5.61	3/0.38									
D2-105.53	DVDP 2	Bas	12.13	6.02	2/0.03	89.1	5.27	4/0.14								-0.76	1252
D2-76.38	DVDP 2	Pht	3.72	5.66	,			,									
D2-45.86	DVDP 2	Pht	2.67	5.48	2/0.39												
D2-61.23	DVDP 2	Тер	2.07	5.49	2/0.24												
EREBUS I	INEAGE																
83435	C. Barne	Bas	6.77	5.34*		79.8	5.41	2/0.27								0.07	UR
83437	Fang	Bas	4.92	6.35		,,,,		2, 0.2								0.07	011
AW82044	Turks Head	Bas	4.74	4.62		83.5	5.42	2/0.31	53.5	5.59		-0.17	>1400	0.97	640	0.80	UR
79300	C. Barne	Bas	4.69	5.28				_,		-10-							
83432	Fang	Bas	4.21	4.42	2/0.19												
83409	Inaccess. Is	Pht	3.47	6.10	_,	80.7	5.91	3/0.03	48.4	6.50	2/0.39	-0.59	>1400	0.40	877	-0.19	>140
AW82038	Turks Head	Pht	3.13	5.06	2/0.18	68.8	5.10	,	57.1	6.00	3/0.37	-0.90	1252	0.94	640	0.05	UR
83415	Tent Is.	Pht	3.00		_,	72.8	5.26		50.0	6.34	-,	-0.72	>1400				
7713	Turks Head	Pht	2.79			64.8	5.39	2/0.22	50.2	6.18		-0.79	1393				
83417	Tent Is.	Pht	2.51	5.61		64.6	5.00	,	42.7	5.96	3/0.32	-0.96	1260	0.35	1075	-0.61	1396
83410	Inaccess. Is.	Tep	2.20	4.55					43.5	5.31	2/1.58			0.76	660		
AW82015	Turks Head	Тер	1.81			55.5	4.50	2/0.31	32.6	5.95	,	-1.46	1000				
83452	Bomb Pk.	Phon	1.64	5.86	2/0.13			,	15.1	5.99				0.13	>1400		
83446	C. Royds	APh	1.30	5.55		57.1	4.63		21.4	5.63	2/1.05	-1.00	1307	0.07	>1400	-0.92	1086
83448	C. Royds	APh	1.23	5.61	2/0.11	57.4	5.03	2/0.41	23.9	5.89	3/0.16	-0.86	>1400	0.28	1109	-0.58	1350
80020	3 Sister	APh	0.99		,			,	18.9	6.02	,						
83400	C. Evans	APh	0.95	6.26	2/0.35	50.2	3.83	4/0.18	20.0	5.81	2/0.49	-1.98	866	-0.45	UR	-2.43	563
97018	Erebus	Aph(b)	0.88	5.68*	,	51.6	3.99	2/0.42	21.4	6.03	3/0.36	-2.04	850	0.35	956	-1.69	828
82146	Erebus	Aph(b)	0.82						16.0	5.98	2/0.08						
Jan-04	Erebus	Aph(b)	0.82						16.0	5.96	2/0.04						
84505	Erebus	Aph(b)	0.82	5.54	2/0.13				16.0	6.02	2/0.13	0.48	<650				
85010	Erebus	Aph(b)	0.82	5.82	2/0.01				16.0	6.12	2/0.12	0.29	763				
86024	Erebus	Aph(b)	0.82						16.0	6.18	2/0.08						
EB06-03	Erebus	Aph(b)	0.82	5.75		51.8	4.27		23.5	6.20	3/0.15	-1.72	948	0.45	1000	-1.48	800
EB06-03	Erebus	Aph(b)	0.82	5.73*													
82403	Erebus	Xeno	2.50						17.7	5.25							
ENRICHE	D FE SERIES	(EFS)															
AW82033	Turks Head	TrAnd	3.89			77.1	5.13		50.7	5.92	2/0.14	-0.79	>1400				
83412	Inaccess Is.	TrAnd	1.57	4.82													
AW82023	Lewis Bay	TrAnd	1.35	5.92	2/0.25	44.7	4.43									-1.49	831
83407	Inaccess Is.	Phon	0.37	5.71	2/0.38	21.3	4.13		10.1	5.88		-1.75	950	0.17	996	-1.58	996
82405	Bomb Pk.	Tr	0.14						3.2	6.88	3/0.30						

APh-anorthoclase phonolite, Aph(b)-anorthoclase phonolite bomb, Bas-basanite, Pht-phonotephrite, Phon-phonolite, Tep-tephripholite, Tr-Trachyte, TrAnd-trachyandesite, Xeno-xenolith * Analyzed by laser ablation.

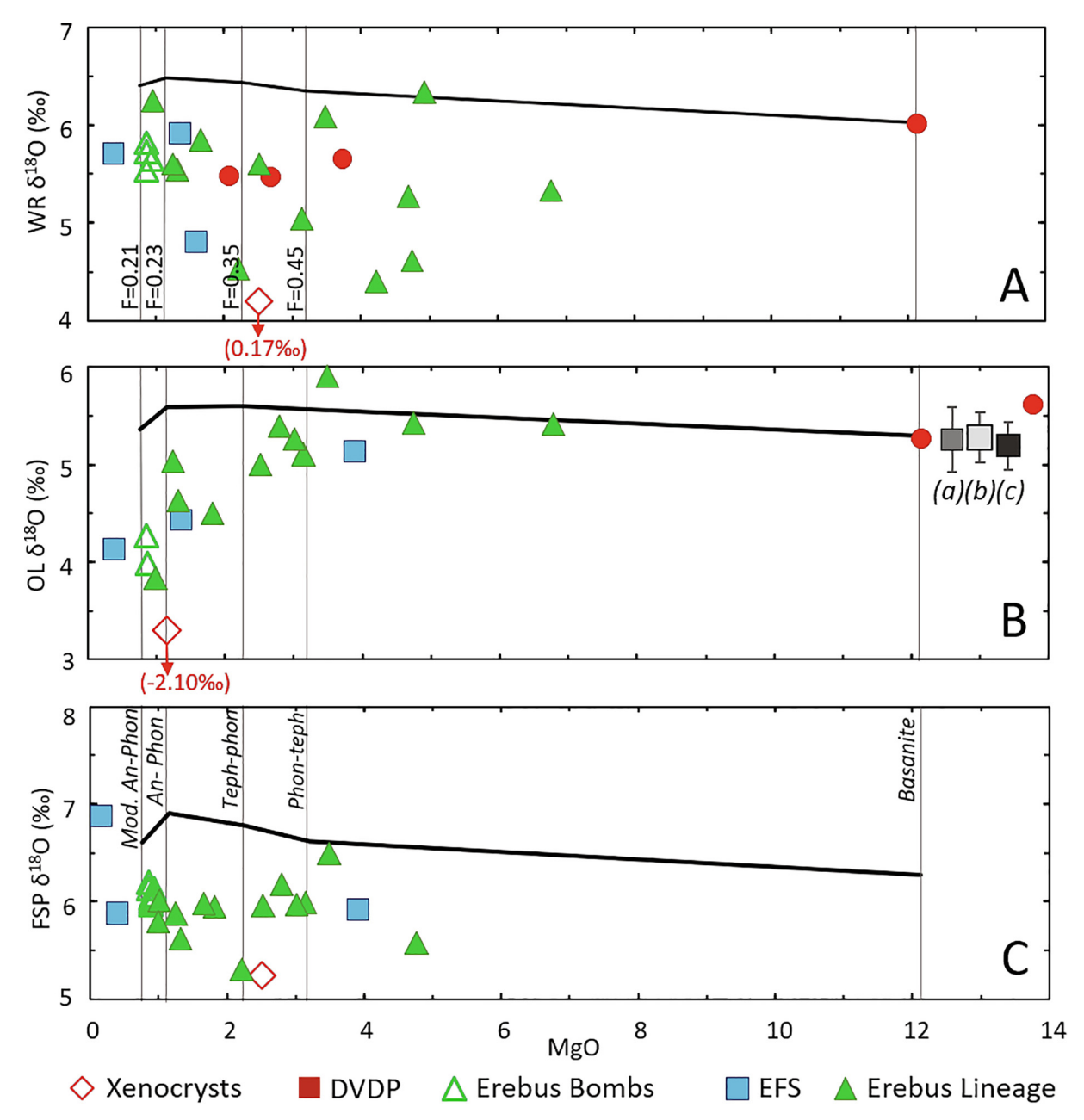


Fig. 2. Measured δ^{18} O values (as % VSMOW): (A) whole rock (WR) and glass; (B) olivine (OL); and (C) feldspar (FSP). Plotted against the MgO content (in wt%) of the whole rock and glass samples. Erebus lineage (filled green triangle), DVDP lineage (red dot), enriched iron series (EFS) lavas from the Erebus center (blue filled square), recent anorthoclase phonolite bombs erupted from Erebus volcano (open green triangle) and xenoliths (open red diamond). Modeled δ^{18} O fractionation trend for the Erebus lineage starting from an assumed parental basanite (DVDP 2-105.53) is shown by black line. Corresponding trends for olivine and feldspar were calculated and averaged at progressively lower fractionation temperatures (Chiba et al., 1989; Chacko et al., 2001; Eiler, 2001; Zhao and Zheng, 2003). In (B) δ^{18} O values of olivines in primitive alkalic basaltic rocks in northern Victoria Land, Antarctica from (a) Perinelli et al., (2006); (b) Nardini et al. (2009) and (c) Panter et al. (2018). Vertical line with F values refer to weight fraction of products from mass balance model of crystal fractionation starting from the parental basanite (DVDP 2-105.53).

0.17%, respectively (Table 1). These low $\delta^{18}O$ values give insight into conditions in a sub-volcanic magma chamber in the vicinity of Erebus.

Nineteen olivine samples were analyzed and have $\delta^{18}O$ ranging from -2.10 to 5.91% (Table 1). There is a pronounced depletion of $\delta^{18}O$ with decreasing MgO (Fig. 2B)

and Fo content (Fig. 4B). Olivine in the more mafic samples (MgO > 4 wt%) has an average oxygen isotope composition of $5.42 \pm 0.14\%$ (n = 4) and the parental basanite DVDP 2-105.53 olivine has a δ^{18} O of 5.26%. These basaltic olivine oxygen isotope values are like Late Cenozoic alkalic basalts in northern Victoria Land, Antarctica (Perinelli et al., 2006;

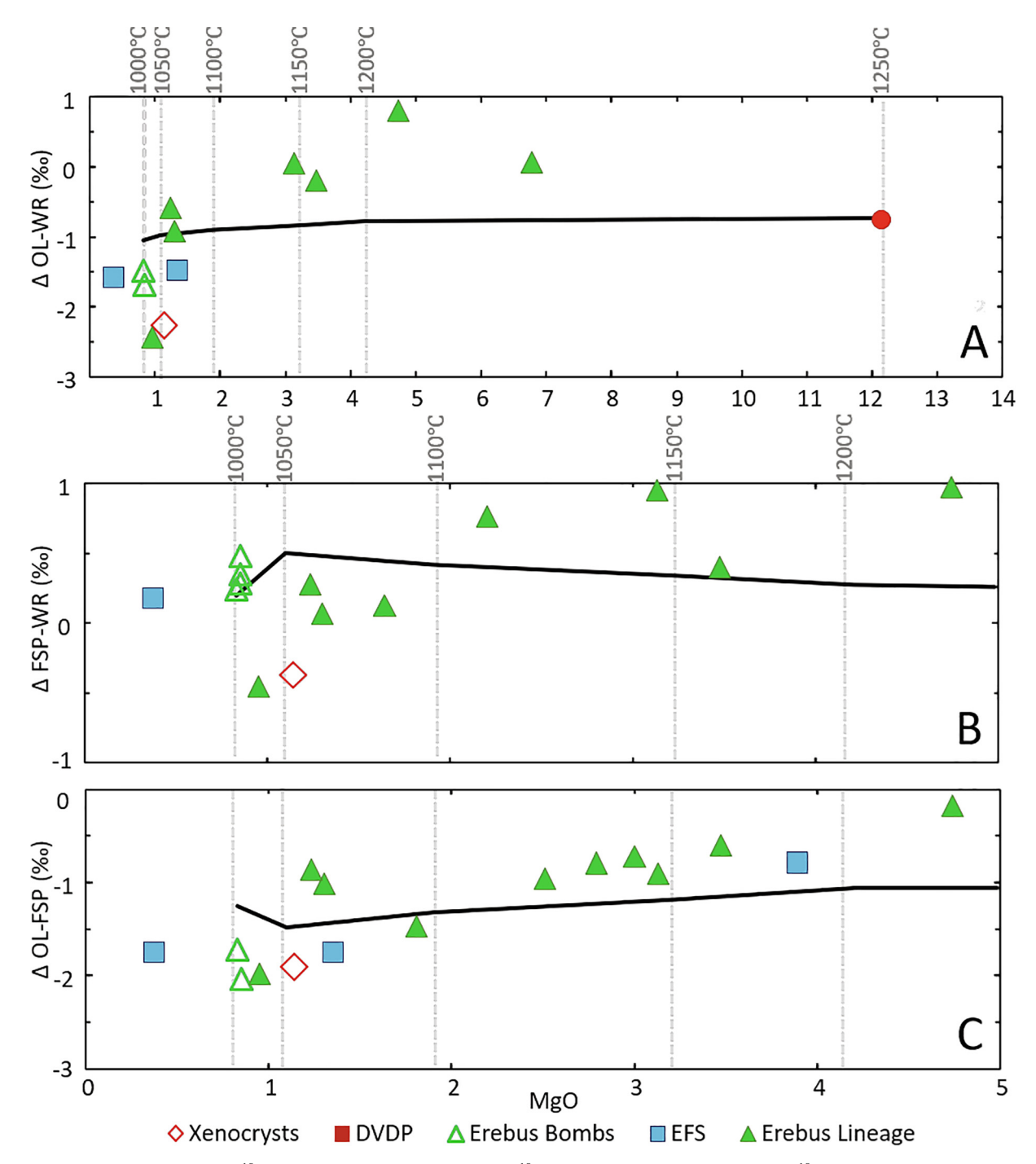


Fig. 3. Fractionation factors ($\Delta^{18}O(a-b)$) for analyzed samples. (A) $\Delta^{18}O(Olivine-Whole rock/Glass)$; (B) $\Delta^{18}O(Feldspar-Whole rock/Glass)$. (C) $\Delta^{18}O(Olivine-Feldspar)$. Trend lines show modeled temperature-dependent fractionation factors. Temperatures (°C) used to calculate modeled $\Delta^{18}O(min-melt)$ for each stage of fractionation are shown.

Nardini et al., 2009) and from the NW Ross Sea (Panter et al., 2018). They are also within the range of δ^{18} O measured in the HIMU mantle (Eiler, 2001) and mantle olivine (Mattey et al., 1994; Dallai et al., 2003).

Feldspar in lava samples has a relatively narrow range of $\delta^{18}O$ from 5.3 to 6.5% with a weak trend of decreasing $\delta^{18}O$ with decreasing whole rock MgO (Fig. 2C). Anorthoclase in historically erupted bombs from Erebus have $\delta^{18}O$

ranging from 5.96 to 6.20 and overall uniform oxygen isotopic composition with a mean and standard deviation of $6.07 \pm 0.19\%$ (n = 7).

In the enriched-Fe series (EFS) (Table 1) trachyandesites and phonolite whole-rock samples $\delta^{18}O$ ranges between 4.82 and 5.92%. Olivine shows a systematic decrease of $\delta^{18}O$ from 5.13 to 4.13 with increased evolution of the magmas as MgO decreases from 3.89 to 0.37 wt%. The feldspars

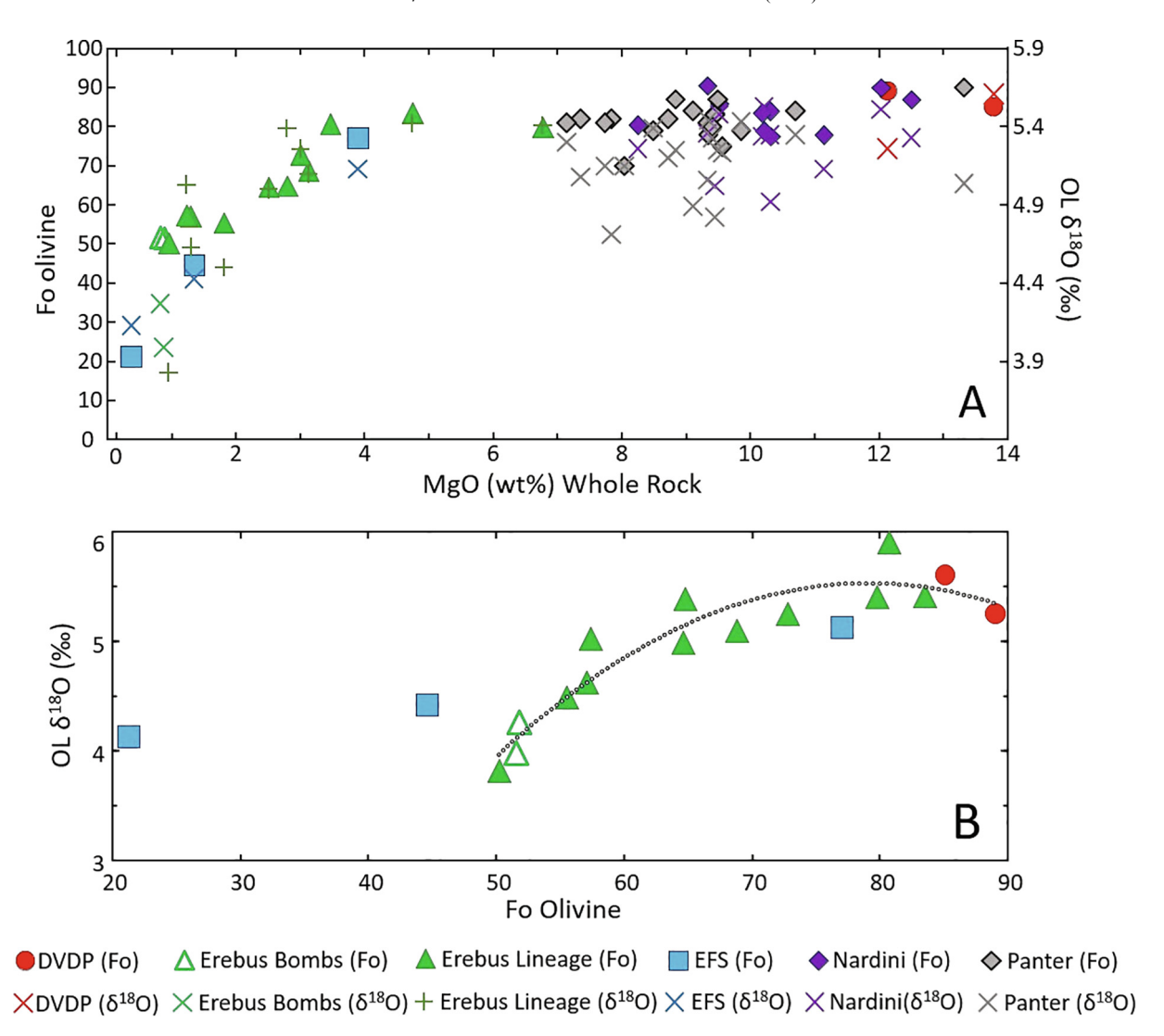


Fig. 4. A Variation of olivine forsterite contents (Fo %) (solid symbols) (left axis) and $\delta^{18}O$ (crosses and + symbols) (right axis) with the whole rock/glass MgO content. Olivine from northern Victoria Land basalts (Nardini et al., 2009), illustrating similar correlation between $\delta^{18}O$ and forsterite content with the bulk MgO content of the samples. (B) Plot of $\delta^{18}O$ of olivines (OL) vs. forsterite (Fo) content show a strong polynomial relationship $y = -0.0019x^2 + 0.3036x - 6.4063$; R = 0.89. EFS olivines (blue filled squares) show a linear trend which diverge from that shown by the EL and DVDP lineage samples.

 δ^{18} O range between 6.88 and 5.88‰, mostly like feldspars in Erebus lineage intermediate samples. An EFS trachyte from Bomb Peak (82405) has the most enriched feldspar with a δ^{18} O of 6.88 (Fig. 2C).

5. DISCUSSION

5.1. Geothermometry

Temperatures calculated from $\Delta^{18}O(\text{min-melt})$ and $\Delta^{18}O(\text{olivine-feldspar})$ (Table 1) are based on models by Chiba et al. (1989) and Zhao and Zheng (2003) and data compiled by Eiler (2001). The feldspar-melt equilibrium temperatures for a phonolite bomb sample EB06-03 is 1000 °C. This agrees with the 1000 °C temperature measured at the Erebus lava lake by Fourier transform infrared spectroscopy (FTIR) (Calkins et al., 2008) and Fe-Ti

geothermometry (Kelly et al., 2008). Temperatures ranged from <600 to >1400 °C for samples of intermediate compositions. Nonsensical calculated temperatures indicate prominent disequilibrium at certain sample locales including Turks Head and Inaccessible Island. An olivine whole rock temperature calculated for DVDP2-105.53 was 1252 °C, which falls within the expected range for basanites at >8 kbar depth (Oppenheimer et al., 2011) and entrapment temperatures of 1184 ± 28 °C (n = 87) based on melt inclusions from Ross Island basanites (Rasmussen et al., 2017).

Anorthoclase phonolite lava samples 83,446 and 83,448, have equilibrium temperatures ranging from >1400 to 1086 °C (Table 1) which are higher than would be expected for such an evolved magma resulting from high degrees of fractionation in the Erebus lineage. These older anorthoclase phonolite lavas are compositionally similar to the

phonolite in the lava lake which has a measured temperature of 1000 °C. It is possible that these older lava samples fractionated, away from the main magma chamber and at higher temperatures than those observed in the lava lake.

5.2. Predicted fractionation trends

Olivine has a uniform oxygen isotope composition in samples with MgO contents ranging from 14 to 3 wt% (Fig. 2B). However, in samples with \leq 3 wt% MgO contents the δ^{18} O decreases significantly in the olivine. This trend is inconsistent with fractional crystallization being the only control in the magmatic evolution of the Erebus lineage.

Mass balance fractional crystallization models (Kyle et al., 1992) show that the evolved anorthoclase phonolite magmas on Erebus represent a 0.23 weight fraction of a parental basanite melt. Using these models, we develop Rayleigh distillation oxygen isotopic fractionation models for melt, olivine and feldspar. The assumed starting parental basanite (D2-105.53) has a whole rock δ^{18} O of 6.02‰. Calculated δ^{18} O values for the 4 stages (Fig. 2) were calculated based on 1000ln α (min-melt) by Clayton et al. (1989), Chiba et al. (1989), Eiler (2001), and Zhao and Zheng (2003). The calculations are given in Table S6. The fractionation models predict a slight increase in δ^{18} O for melt (Fig. 2A), olivine (Fig. 2B), and feldspar (Fig. 2C) with increasing degrees of fractional crystallization and the resulting decreasing MgO contents. The trends of increasing δ^{18} O from the parental basanite to the phonolite are due to the strong crystallization and fractionation of depleted δ¹⁸O minerals such as olivine, Fe-Ti oxides, and clinopyroxene. We calculated a 4th stage model, from F = 0.23 to F = 0.21 to observe the effects of the fractionation of the anorthoclase megacrysts, magnetite and degassing of CO₂ from the phonolite magma present in the Erebus lava lake. Crystallization of isotopically enriched anorthoclase feldspar (An22) in this final stage resulted in a slight depletion of whole rock δ^{18} O (Fig. 2).

The measured olivine, feldspar and whole rock/glass oxygen isotope compositions (Table 1) are strongly lowered compared to the modeled fractionation trends for the entire Erebus lineage (Fig. 2). In the phonolite bombs, the measured anorthoclase feldspar oxygen isotopes compositions are over 1.0% lighter, olivine compositions 1.8% lighter, and glass are nearly 0.8% lighter than the model values. Measured olivine δ^{18} O values form a continuous depletion trend with increased fractionation for magmas with less than 4 wt% MgO (Fig. 2B).

To investigate these depletions, we compared $\Delta^{18}O$ of olivine–feldspar and mineral–melt pairs to determine the apparent disequilibrium for each stage of fractionation (Table 1, Fig. 3). Fractionation factors $\Delta^{18}O(a-b)$ were modeled at estimated temperatures for each stage and compared to actual $\Delta^{18}O$ of mineral–melt pairs from the Erebus lineage (Fig. 3). Comparison to models indicated disequilibrium between olivine-melt (Fig. 3A) and feldspar-melt (Fig. 3B) in the Erebus lineage for most intermediate stages from basanite through tephriphonolite (MgO = 7.0 thru 1.8 wt%). Predicted values of $\Delta^{18}O$ (feldspar–melt) were small to negligible for the glass and anorthoclase in the

bombs at temperatures of 1000 °C. This shows there is oxygen isotope equilibrium between the feldspar and the phonolite melt. Such equilibrium in bomb samples agrees with long residence time of anorthoclase phenocrysts in the currently openly convecting lava lake and the compositional invariance of the lava lake in historic times (Reagan et al., 1992; Kelly et al., 2008; Sims et al., 2008; Moussallam et al., 2015). Fractionation between olivine and other phases, however, exhibited much stronger disequilibrium during intermediate petrologic stages. Actual values of Δ^{18} O(olivine-melt) only converged toward predicted values in the initial differentiation stages that formed the phonolite melts at 1050 °C (Fig. 3A). In summary, it appears that olivines maintained strong disequilibrium with the melt following fractionation from the parental basanite, resulting in strongly depleted δ^{18} O olivine values superimposed on a systematic depletion influencing the entire system.

5.3. Trends in $\delta^{18}O$ depletion

As discussed above, olivine compositions in the Erebus lineage formed an overall trend of decreasing $\delta^{18}O$ with increasing fractionation (Fig. 4). A correlation is observed between the olivine Fo values and their measured $\delta^{18}O$ for the Erebus and DVDP lineage samples and for olivine from less differentiated Cenozoic basalts in northern Victoria Land (Nardini et al., 2009; Panter et al., 2018) (Fig. 4B). This correlation suggests that factors other than simple fractionation of the melt affected both olivine MgO:FeO ratios and their oxygen isotopic content.

The isotopic depletions observed in the DVDP and EFS samples are like the EL samples and exhibited apparent decrease in $\delta^{18}O$ as the magmas evolved. EFS olivines also displayed a steady decrease in $\delta^{18}O$ with decreasing Fo content (Fig. 4), supporting a common mechanism that affected all regional samples similarly, although possibly not to the same extent.

Departures of some samples of the Erebus lineage from the overall trends (Fig. 2) may help elucidate the unique factors responsible for this overall depletion. Samples from Inaccessible Island (83,410 and 83,409), part of the Delbridge Islands, exhibited systematically high $\delta^{18}O$ values for both olivines and feldspars, whereas those from Turks Head (AW82044 and 7713) exhibited strong disequilibrium between melt phases. Esser et al. (2004) identified a nonlinear Mg# $[100 MgO/(MgO + FeO^*)]$ vs. $^{40}Ar/^{39}Ar$ age trend among the Delbridge Islands succession, including Inaccessible Island, Turks Head, and Tryggve Point, indicating that these lavas evolved in a magma chamber separate to that of Erebus. These eruptive centers may have been active for as little as 150 ka (Esser et al., 2004); thus, they would have evolved at an accelerated pace (Moore and Kyle, 1987) under unique pressure and temperature conditions, isolating them from the specific factors that depleted the main Erebus lineage.

5.4. Effects of a heterogeneous mantle

Much speculation surrounds the presence or absence of a mantle plume to explain the volcanism at Erebus volcano

and rift activity in the western Ross Sea (Kyle et al., 1992; Rocchi et al., 2002, 2005; Phillips et al., 2018; Day et al., 2019; Martin et al., 2021). Heterogeneous mantle sources are often suggested to explain variations in isotopic or chemical compositions of volcanic products (e.g., Zindler and Hart, 1986; Hofmann, 2003). A mantle plume could easily provide a unique source of depleted δ^{18} O magma; however, a depleted mantle source could not explain the systematic depletion of the differentiated melts with time. Isotopic compositions of mantle xenoliths located in southern Ross Sea indicate a source with a significant HIMU mantle component (Martin et al., 2021). DVDP 2-105.53 isotopic analyses fall within this range (Sims et al., 2008), verifying the DVDP basanite as a likely parental representation of the Erebus lineage; however, this does not need to be the case. A low δ^{18} O magma could represent the parental end-member, or our limited sampling of the DVDP basanite could be an erroneous representation of the isotopic composition of this melt. In any case, a wholly lowered starting point for this system could not explain the trend of temporal depletion encountered.

5.5. Degassing of CO₂

Fractionation factors for magmatic degassing Δ (meltgas) are upward of several tenths of a per mil at magmatic temperatures (Eiler, 2001), implying a possible important source for isotope depletion. Oxygen isotope fractionation by degassing requires near-complete degassing of a melt's CO₂ and H₂O to lower the δ^{18} O whole rock value by 0.5%.

Olivine-hosted melt inclusions from nine basanites sampled on Ross Island at vents surrounding Erebus have CO₂ contents of 0.2-1.8 wt% (Rasmussen et al., 2017). These basanites are considered representative of those feeding the Erebus magmatic system and it can be expected that the CO₂ content of the parental Erebus basanites was exceedingly high, possibly on the order of 1.5 wt%. However, on Erebus olivine-hosted melt inclusions from more evolved rocks have lower CO2 contents of 0-0.2 wt% indicating shallow (<6 km) crystallization in high level magma storage reservoirs (Rasmussen et al, 2017). At Erebus, the measured CO₂ degassing rate is ~1330 Mg/day (Oppenheimer and Kyle, 2008b). This suggests deepseated magmatic sources provide a constant stream of CO₂ possibly from the mantle to the convecting lava lake (Oppenheimer and Kyle, 2008b; Oppenheimer et al., 2011).

We present two models for open system degassing of CO_2 from a theoretical basanite melt at 4 kbar. Complete degassing of 4080 km³ of basanite melt with 0.06 wt% CO_2 predicted a maximum depletion of 0.02‰ of the original melt, insufficient to cause the observed depletions (Fig. 5). Open-system degassing assuming continuous replenishment of CO_2 from a deeper source with values of 7.58‰ (assuming fractionation from a $\delta^{18}O$ of 5.2‰ at 1300 °C) and continuous degassing at current, measured rates for 1300 ka since the initial stages of construction of Mt. Erebus would achieve upwards of 0.11‰ depletion of the primary melt due to Rayleigh fractionation at lower magma-chamber temperatures. This process of long-term CO_2 degassing could be a minor contributor to the current

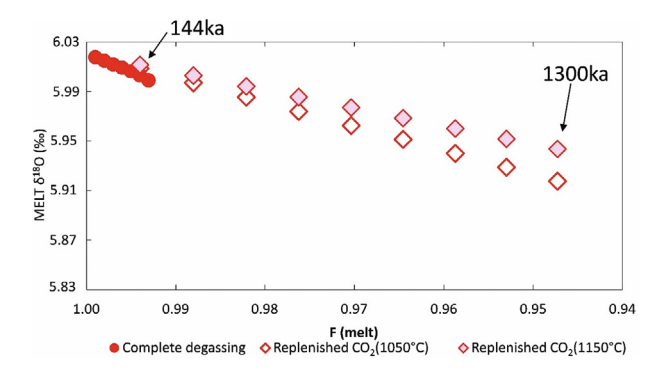


Fig. 5. Isotopic depletion of melt assuming open- and closed-system degassing of CO_2 in an intermediate depth magma chamber. Closed-system degassing is estimated at progressively decreasing fractionation temperatures from 1250° to 1000 °C. Complete degassing of the original volume of basanite melt required for the formation of Erebus magmas would conclude in 144 ka. Open system degassing at current flux rates assuming completely replenishable concentrations of CO_2 dissolved in an intermediate magma chamber were modeled at temperatures of 1050 °C and 1150 °C. Optimistic calculations at 1050 °C predicted a final melt composition of 5.83% following 1.3 Ma of continuous degassing.

depletion of modern Erebus glasses with $\delta^{18}O$ values of 5. $7 \pm 0.15\%$. Fractionation of CO_2 from the melt at even lower temperatures (<1050 °C) and doubling the flux of CO_2 could increase this depletion even more.

Several caveats, however, are inherent to this model. The calculations do not account for isotopic enrichment due to Rayleigh distillation of crystallization products over time, predicting a 0.4% increase in δ^{18} O values over the primary melt and effectively cancelling out any depletion due to continuous degassing. In addition, the assumption that continuous degassing at present rates for the duration of Erebus' construction is largely untested and generally considered a unique manifestation of the current open-system lava lake. Similarly, observed isotopic depletions in EFS and DVDP lavas would require the same mechanism of open-system fluxing of CO₂ over time to replicate this effect. Measurements of continuously decreasing δ^{18} O of CO₂ in melt inclusions for the Erebus lineage and similarly depleted δ¹⁸O of presently degassing CO₂ from the summit crater could verify this model.

5.6. Assimilation of cumulates or hydrothermally altered edifices

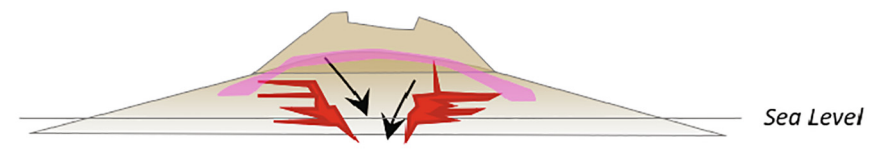
Subsurface scavenging of cumulate olivines has been invoked to explain small depletions for low $\delta^{18}O$ at Galunggung volcanoes (Harmon and Gerbe, 1992). Such models involve sidewall melting and scouring of the crystalline roof into the shallow magma chamber. Significant remelting of high-Fo cumulates could cause depletion of the melt; however, this process would be limited by the isotopic composition of the incorporated material. There is no evidence of xenocrystic forsteritic-rich olivine in Erebus intermediate and phonolitic lavas so we do not consider this an explanation for the low oxygen isotopic compositions of the whole rocks/glass and mineral phases.

Assimilated material with even greater depletions, however, could be derived from hydrothermally altered volcanic edifices (Troch et al., 2020). This has been proposed for Hawaii (Wang et al., 2003; Wang and Eiler, 2008), the Skaergaard Intrusion (Bindeman et al., 2008), Yellowstone

(Bindeman and Valley, 2001) and has become the norm to explain low δ^{18} O silicic magmas (Troch et al., 2020). All volcanoes are host to some form of hydrothermal system, even immature ones characterized as exhibiting a low water:rock ratio (Hedenquist, 1986). The occurrence of

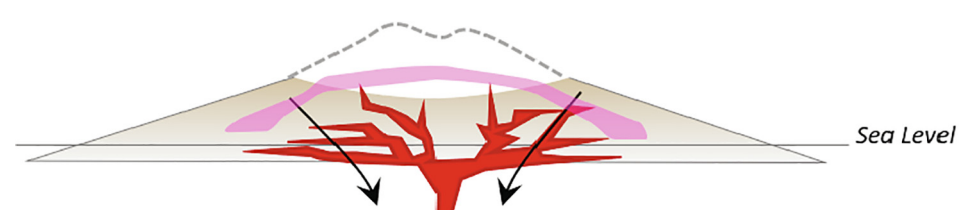


Stage 1 – Early basanite evolution during proto-Erebus shield building phase. During initial subaerial phase, hydrothermal alteration with meteoric water is negligible.

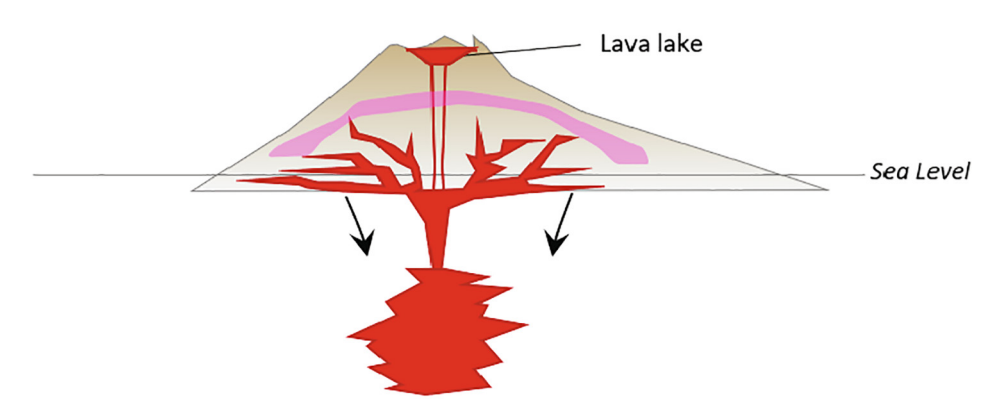


Stage 2 – Phonotephrite evolution, steeper cone forms on slopes of proto-Erebus volcano, followed by caldera forming event which destroys summit.

Larger degrees of crustal contamination with hydrothermally altered units are incorporated following major collapses. Equilibration of melt in intermediate magma chamber, olivines are slow to equilibrate due to slower diffusion.



Stage 3 – Transition from tephriphonolite to phonolite, building of modern Erebus cone. Hydrothermal system is more mature, additional collapse events of modern Erebus caldera means greater crustal contamination with hydrothermally altered units. Equilibration of melt in intermediate magma chamber, olivines reach equilibrium with melt.



Stage 4 – Modern Erebus anorthoclase phonolite lavalake. Melt reaches lava lake for period of repose, additional crystallization of magnetite increases the melt $\delta^{18}O$. Olivines are slow to equilibrate with new melt $\delta^{18}O$ due to diffusion; magnetite fractionation would result in slight decrease of olivine signature as well.

Fig. 6. Cartoon illustrating incorporation of hydrothermally altered volcanic edifice (shown in pink) through the various Erebus building phases. (For interpretation of the references to colour in this figure legend, the reader is referred to the web version of this article.)

multiple ice caves around the summit crater (Ilanko et al., 2019) is evidence of structural pathways for the formation of hydrothermal cells at depth. Ilanko et al., (2019) showed that gas emissions from fumaroles on the floors of the ice caves are mainly air but with varying amounts of volcanic CO₂. The chemistry of the fumarolic gases requires temperatures of 120 °C and a hydrothermal system at depth.

Significant crustal contamination in the main Erebus lineage is not discernible from radiogenic isotopes or trace elements (Kyle et al., 1992; Sims et al., 2008; Phillips et al., 2018). Yet, hydrothermal alteration by meteoric water can

change the oxygen isotopic composition of rock without altering its bulk chemical composition, including trace elements and radiogenic ⁸⁷Sr/⁸⁶Sr signatures (Taylor, 1979; Bindeman, 2008). Incorporation of altered volcanic units in shallow crustal environments is aided by continual caldera collapses and buildup of the volcanic edifice, which brings the altered units deeper towards the melting zone (Fig. 6). Hydrothermal alteration also aids with volatile flux to support re-melting and mechanical incorporation of the glassy, porous units (Bindeman, 2008). The extremely depleted nature of Antarctic meteoric precipitation (Masson-Delmotte et al., 2008) would result in significant

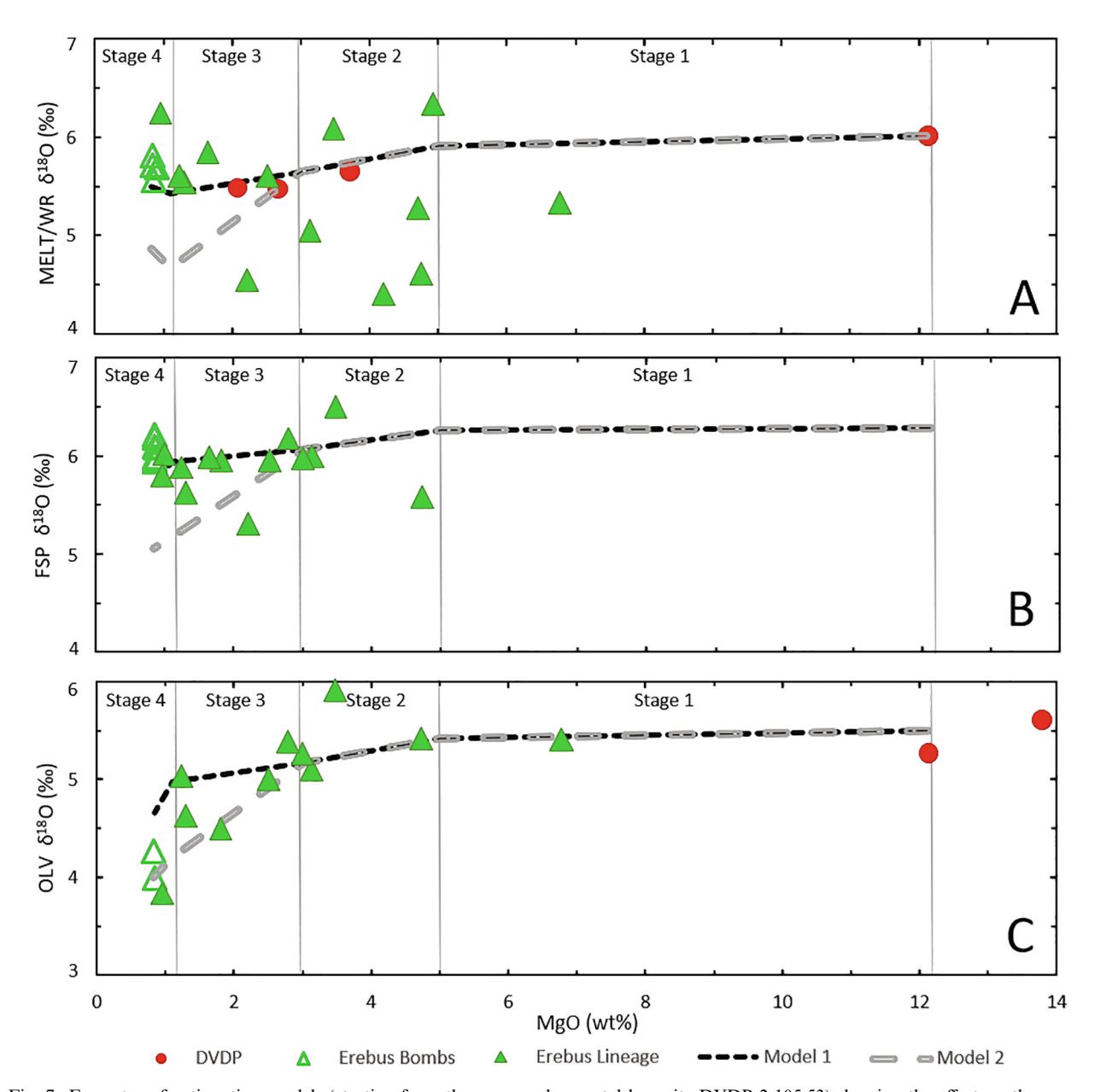


Fig. 7. Four stage fractionation models (starting from the presumed parental basanite DVDP 2-105.53) showing the effect on the oxygen isotopes of (A) WR/Melt, (B) Feldspar (FSP) and (C) Olivine (OL) by incorporation of 7.7% (model 1) and 11% (model 2) of altered volcanic edifice. In model 1 the resulting values agree with the observed δ^{18} O in melt, olivine and feldspar pairs through Stage 4 except for olivine in recently erupted anorthoclase phonolite bombs. In model 2 the greatest effects occur in stages 3 and 4 during the evolution of phonolite from tephriphonolite. The model calculations are given in Supplemental Tables S7 and S8.

decrease in isotopic compositions of the altered units with much smaller water-rock ratios.

Two phonolitic xenoliths (samples 82,403 and 82,431, Table 1) give insight into the high-level magma chamber (s) at Erebus. Anorthoclase feldspar in sample 82,403 has a $\delta^{18}O$ of 5.25 slightly lower than most of the other analyzed feldspar. On the other hand, sample 82,431 has extremely low $\delta^{18}O$ with WR, olivine and feldspar values of 0.17, -2.10 and -0.2, respectively. These low $\delta^{18}O$ clearly indicating assimilation of hydrothermally altered material or interaction with hydrothermal fluids derived from the local snow.

Using a closed-system box model (Table S7) oxygen isotopic composition of sample 82,431 could result from enrichment of a phonolite with a $\delta^{18}O$ of 5.68% by -35% Antarctic water with a minimum 1–3.5 water:rock ratio. Two fractionation models are presented that involve the increasing incorporation of low $\delta^{18}O$ materials into the fractionating melt (Fig. 7). A total 11.0% contribution of altered material over time is needed to produce the modern olivine compositions; a 7.7% contribution is needed to produce the modern anorthoclase phonolite melt (Table S8).

5.7. Low δ^{18} O in olivines

Olivine is often used as the sole proxy for monitoring isotopic trends in melts. As olivine is refractory this limits oxygen diffusion. The simple Fe–Mg solid solution in olivine results in negligible potential reequilibration (Eiler, 2001; Bindeman, 2008). We observed a disequilibrium between olivine and melt (whole rock/glass) and feldspar at most stages of fractional crystallization (Table 1) and, most notably, in the recently erupted anorthoclase phonolites bombs (Fig. 7). The systematic depletion of whole rock/glass compositions may be caused by various geologic factors described above; however, these alone cannot explain the decrease of δ^{18} O in the olivine.

We propose a two-stage model of equilibration (Fig. 6). The first in an intermediate-depth magma chamber where altered materials is incorporated forming a melt and olivine with lower δ^{18} O. The phonolite resides in the convecting lava lake and the connected high level magma reservoir where anorthoclase megacrysts grow over the course of 10¹⁻² yrs prior to eruption (Moussallam et al., 2015). Olivine phenocrysts may not have enough time to reequilibrate their O-isotopic values via diffusion and thus record a lower δ^{18} O phase within the shallow magma reservoir. The coincidence of strong olivine Δ^{18} O disequilibrium during the formation of the modern anorthoclase-rich phonolite melt and shallow lava lake argues for differential isotopic fractionation between the various mineral phases. The variability between modern olivine δ^{18} O values amongst different samples, where MgO wt% <2, also supports a heterogeneous or sporadic process for which low δ^{18} O olivines are incorporated into the modern assemblage.

Fayalitic olivines (Fa₅₀) have low abundances in the anorthoclase phonolite bombs occuring as smaller, subhedral phenocrysts. Microprobe analyses of the olivine (Kelly et al., 2008), have not identified zoning or unique rim compositions that would indicate partial

re-equilibration in the shallow magma chamber. Diffusion of oxygen in olivines is slow and estimated to take ~126 ka for a 2 mm long olivine to re-equilibrate with its host melt's δ^{18} O composition (Ryerson et al., 1989; Bindeman, 2008). Chemical variations have not been found in olivine undergoing oxygen diffusion (Bindeman, 2008) unless undersaturation calls for resorption, thus leaving little chemical indication for such a process without single crystal isotopic transects. At Erebus, the olivine δ^{18} O is coupled with their Fo contents. Oppenheimer et al. (2011) observed a marked decrease in the fO₂ composition of the shallow lava lake in comparison to melt inclusions from a magma chamber at intermediate depths. This phenomenon was attributed to buffering by FeO and increased magnetite precipitation in the shallow chamber. It is possible that olivine isotopic compositions are strongly affected by decreasing oxygen fugacity in either an intermediate depth magma chamber or shallower magma reservoir. These arguments may be addressed by olivine crystallization studies in the presence of changing volatile compositions.

6. CONCLUSIONS

At Erebus volcano whole rocks/glass, olivine and feld-spar exhibit a trend of decreasing $\delta^{18}O$ values with increased fractional crystallization. A primitive basanite lava assumed to be representative of the parent for the Erebus magmatic lineage, has whole rock and olivine $\delta^{18}O$ of 6.02‰ and 5.26‰, respectively. This is consistent with their HIMU mantle source. Recently erupted anorthoclase phonolites bombs have feldspar, melt, and olivine $\delta^{18}O$ of 6.0‰, 5.7‰, and 4.0‰, respectively. Using geochemical mass balance models of fractional crystallization forward models show calculated $\delta^{18}O$ increase in the magmatic systems. The opposite to that observed. Feldspar phenocrysts appeared to be close to isotopic equilibrium with the melt throughout the magmatic evolution. Olivine is in disequilibrium with the melt and feldspars throughout.

Scavenging and incorporation of altered and isotopically depleted volcanic edifice through an intermediate magma chamber is proposed as a possible cause for the observed isotopic trends. Extremely isotopically light Antarctica snow would result in lower δ^{18} O values for the shallowly intruded magmas with little contribution from mass. A water-to-rock mass ratio of approximately 1:4 and geothermal temperatures of 300 °C explain the isotopically light phonolite xenolith observed at Erebus. Incorporation of 7.7-11% altered material over time are required to produce the modern isotopic depleted melts. Strong Δ^{18} O disequilibrium between olivine/melt and feldspar/melt pairs correlates strongly with the modern evolution and formation of phonolite magmas at Erebus. Olivine isotopic compositions correlated strongly with their forsterite contents indicating additional unique factors influencing them. Differential precipitation of olivine in the intermediate magma chamber and feldspar in the shallow lava lake may result in depleted olivine in the modern mineral assemblage if olivine are slow to equilibrate their isotopic composition via diffusion. Other factors controlling the fO2 may also cause olivine disequilibrium.

Continuous degassing of CO_2 from basanite melts in the mantle was also investigated as a possible mechanism to explain the low $\delta^{18}O$ values. Models assuming complete replenishment of the dissolved CO_2 in our melt with mantle values of 7.58‰, followed by Rayleigh fractionation from open system degassing for 1.3 Ma, achieved a final melt composition of 5.92‰; this was still higher than the observed composition of the anorthoclase phonolite glasses.

The abundance of low oxygen-isotope systems may be drastically overlooked in the volcanic record, thus calling for a largely universal method for such depletions which may affect volcanic systems in various geologic and climatic settings. The Erebus lineage lavas offer a unique opportunity to study these mechanisms due to the lack of meteoric precipitation and apparent crustal assimilation. The incorporation of hydrothermally altered volcanic edifice may represent a more common process than previously thought, largely due to the lack of chemical fingerprints related to meteoric alteration of similar volcanic lithologies to the melt. Very little water:rock interaction is required to produce altered units and frequent dome or caldera collapses aid in introducing edifice material into the melt.

Declaration of Competing Interest

The authors declare that they have no known competing financial interests or personal relationships that could have appeared to influence the work reported in this paper.

ACKNOWLEDGMENTS

This work was partially supported by National Science Foundation grants ANT0838817, ANT1142083 and PLR1644234. We thank the 3 journal reviewers (Ilya Binderman, Kurt Panter and Brad Peters) and Associate Editor Rosemary Hickey-Vargas for helpful constructive comments.

APPENDIX A. SUPPLEMENTARY MATERIAL

Supplementary data to this article can be found online at https://doi.org/10.1016/j.gca.2021.06.008.

REFERENCES

- Bindeman I. N. (2008) Oxygen isotopes in mantle and crustal magmas as revealed by single crystal analysis. *Rev. Mineral. Geochem.* **69**, 445–478.
- Bindeman I. N., Brooks C. K., McBirney A. R. and Taylor H. P. (2008) The low δ¹⁸O late-stage ferrodiorite magmas in the Skaergaard Intrusion: Result of liquid immiscibility, thermal metamorphism, or meteoric water incorporation into magma?. *J. Geol.* 116, 571–586.
- Bindeman I. N. and Valley J. W. (2001) Low δ^{18} O rhyolites from Yellowstone: magmatic evolution based on analyses of zircons and individual phenocrysts. *J. Petrol.* **42**, 1491–1517.
- Behrendt J. (1999) Crustal and lithospheric structure of the West Antarctic Rift System from geophysical investigations a review. *Glob. Planet. Change* 23, 25–44.

- Calkins J., Oppenheimer C. and Kyle P. R. (2008) Ground-based thermal imaging of the lava lakes at Erebus volcano, Antarctica. J. Volcanol. Geotherm. Res. 177, 695–704.
- Chacko T., Cole D. R. and Horita J. (2001) Equilibrium oxygen, hydrogen and carbon isotope fractionation factors applicable to geologic systems. Rev. Mineral. Geochem. 43, 1–81.
- Chiba H., Chacko T., Clayton R. N. and Goldsmith J. R. (1989) Oxygen isotope fractionations involving diopside, forsterite, magnetite, and calcite: Applications to geothermometry. *Geochim. Cosmochim. Acta* 53, 2985–2995.
- Clayton R. N., Goldsmith J. R. and Mayeda T. K. (1989) Oxygen isotope fractionation in quartz, albite, anorthite and calcite. *Geochim. Cosmochim. Acta* 53, 725–733.
- Dallai L., Ghezzo C. and Sharp Z. D. (2003) Oxygen isotope evidence for crustal assimilation and magma mixing in the Granite Harbour Intrusives, Northern Victoria Land, Antarctica. *Lithos* 67, 135–151.
- Day J. M. D., Harvey R. P. and Hilton D. R. (2019) Melt-modified lithosphere beneath Ross Island and its role in the tectonomagmatic evolution of the West Antarctic Rift System. *Chem. Geol.* 518, 45–54.
- Eiler J. M. (2001) Oxygen isotope variations of basaltic lavas and upper mantle rocks. In *Stable Isotope Geochemistry. Rev. Mineral.*, 43 (eds. J. W. Valley and D. R. Cole), pp. 319–364.
- Esser R. P., Kyle P. R. and McIntosh W. C. (2004) ⁴⁰Ar/³⁹Ar dating of the eruptive history of Mount Erebus, Antarctica: Volcano evolution. *Bull. Volcanol.* **66**, 671–686.
- Ertchi P. and Silverman S. R. (1951) The determination of the relative abundance of the oxygen isotopes in silicate rocks. *Geochim. Cosmochim. Acta* 1, 317–328.
- Finn C. A., Muller R. D. and Panter K. S. (2005) A Cenozoic diffuse alkaline magmatic province (DAMP) in the southwest Pacific without rift or plume origin. *Geochem. Geophys. Geosyst.* **6**, 1–26.
- Gupta S., Zhao D. P. and Rai S. S. (2009) Seismic imaging of the upper mantle under the Erebus hotspot in Antarctica. *Gond. Res.* 16, 109–118.
- Harmon R. S. and Gerbe M. (1992) The 1982–83 eruption at Galunggung Volcano, Java (Indonesia): Oxygen isotope geochemistry of a chemically zoned magma chamber. *J. Petrol.* **33**, 585–609.
- Harris C., Smith H. S. and le Roux A. P. (2000) Oxygen isotope composition of phenocrysts from Tristan da Cunha and Gough Island lavas: Variations with fractional crystallization and evidence for assimilation. *Contrib. Mineral. Petrol.* 138, 164–176
- Hedenquist J. W. (1986) Geothermal systems in the Taupo volcanic zone; their characteristics and relation to volcanism and mineralisation. In *Late Cenozoic volcanism in New Zealand*. *Bull. Royal Soc. New Zealand*, 23 (ed. I. E. M. Smith), pp. 134– 168.
- Hofmann A. W. (2003) Sampling mantle heterogeneity through oceanic basalts: Isotopes and trace elements. In *Treatise on Geochemistry*. Elsevier, pp. 61–101.
- Iacovino K., Oppenheimer C., Scaillet B. and Kyle P. (2016) Storage and evolution of mafic and intermediate alkaline magmas beneath Ross Island, Antarctica. J. Petrol. 57, 93–118.
- Ilanko T., Oppenheimer C., Burgisser A. and Kyle P. (2015a) Cyclic degassing of Erebus volcano, Antarctica. *Bull. Volcanol.* 77, 56.
- Ilanko T., Oppenheimer C., Burgisser A. and Kyle P. (2015b) Transient degassing events at the lava lake of Erebus volcano, Antarctica: Chemistry and mechanisms. *GeoResJ* 7, 43–58.
- Ilanko T., Fischer T. P., Kyle P., Curtis A. and Sano Y. (2019) Modification of fumarolic gases by the ice-covered edifice of

- Erebus volcano, Antarctica. J. Volcanol. Geotherm. Res. 381, 119-139
- Jordan T. A., Riley T. R. and Siddoway C. S. (2020) The geological history and evolution of West Antarctica. *Nature Rev. Earth Environ.* 1, 117–133.
- Kelly P. J., Kyle P. R., Dunbar N. W. and Sims K. W. W. (2008) Geochemistry and mineralogy of the phonolite lava lake, Mount Erebus volcano, Antarctica: 1972–2004 and comparison with older lavas. J. Volcanol. Geotherm. Res. 177, 589–605.
- Kyle P. R. (1981a) The geological history of Hut Point Peninsula as indicated by Dry Valley Drilling Project holes 1, 2 and 3. In *Dry Valley Drilling Project. Antarctic Research Series*, 33 (ed. L. D. McGinnis), pp. 427–445.
- Kyle P. R. (1981b) Mineralogy and geochemistry of a basanite to phonolite sequence at Hut Point Peninsula, Antarctica, based on core from Dry Valley Drilling Project drillholes 1, 2, and 3. *J. Petrol* **22**, 451–500.
- Kyle P. R. (1990a) Erebus Volcanic Province: Summary. In Volcanism of the Antarctic Plate and Southern Oceans. Antarctic Research Series, 48 (eds. W. LeMasurier and J. Thomson), pp. 81–88
- Kyle P. R. (1990b) McMurdo Volcanic Group Western Ross Embayment: Introduction. In Volcanism of the Antarctic Plate and Southern Oceans. Antarctic Research Series, 48 (eds. W. LeMasurier and J. Thompson), pp. 18–25.
- , 66Kyle, P. R. (ed.) (1994)Volcanological and Environmental Studies of Mount Erebus. Antarctic Research Series, 162 p.
- Kyle P. R., Moore J. A. and Thirlwall M. F. (1992) Petrologic evolution of anorthoclase phonolite lavas at Mt Erebus, Ross Island, Antarctica. J. Petrol. 33, 849–875.
- Martin A. P., Cooper A. F., Price R. C., Kyle P. R. and Gamble J.
 A. (2021) Erebus Volcanic Province, Petrology. In Volcanism in Antarctica: 200 Million Years of Subduction, Rifting and Continental Break-Up. Geol. Soc., London Memoirs, 55 (eds. J. L. Smellie, K. S. Panter and A. Geyer).
- Masson-Delmotte V., Hou S., Ekaykin A., Jouzel J., Aristarain A., Bernardo R. T., Bromwich D., Cattani O., Delmotte M. and Falourd S. (2008) A review of Antarctic surface snow isotopic composition: observations, atmospheric circulation, and isotopic modeling. *J. Climate* 21, 3359–3387.
- Mattey D., Lowry D. and Macpherson C. (1994) Oxygen isotope composition of mantle peridotite. *Earth Planet. Sci. Lett.* 128, 231–241.
- Moore J. A. and Kyle P. R. (1987) Volcanic Geology of Mount Erebus, Ross Island, Antarctica. Proc. NIPR Symp. Antarct. Geosci. 1, 48–65.
- Moussallam Y., Oppenheimer C., Scaillet B., Buisman I., Kimball C., Dunbar N., Burgisser A., Schipper C. I., Andújar J. and Kyle P. (2015) Riding the conduit elevator at Erebus volcano: magma motion and speed recorded by anorthoclase megacrystals. *Earth Planet. Sci. Lett.* 413, 1–12.
- Nardini I., Armienti P., Rocchi S., Dallai L. and Harrison D. (2009) Sr-Nd-Pb-He-O Isotope and Geochemical Constraints on the Genesis of Cenozoic Magmas from the West Antarctic Rift. J. Petrol. 50, 1359–1375.
- Oppenheimer, C. and Kyle, P. (eds.) (2008a) Volcanology of Erebus volcano, Antarctica. Special Issue. J. Volcan. Geotherm. Res.
- Oppenheimer C. and Kyle P. R. (2008b) Probing the magma plumbing of Erebus volcano, Antarctica, by open-path FTIR spectroscopy of gas emissions. *J. Volcanol. Geotherm. Res.* 177, 743–754
- Oppenheimer C., Lomakina A. S., Kyle P. R., Kingsbury N. and Boichu M. (2009) Pulsatory magma supply to a phonolite lava lake. *Earth Planet. Sci. Lett.* **284**, 392–398.
- Oppenheimer C., Moretti R., Kyle P. R., Eschenbacher A., Lowenstern J. B., Hervig R. L. and Dunbar N. W. (2011)

- Mantle to surface degassing of alkalic magmas at Erebus volcano, Antarctica. *Earth Planet. Sci. Lett.* **306**, 261–271.
- Panter K. S. (2021) Petrology and tectonomagmatic overview. In Volcanism in Antarctica: 200 Million Years of Subduction, Rifting and Continental Break-Up. Geol. Soc. London, Mem., 55 (eds. J. L. Smellie, K. S. Panter and A. Gever).
- Panter K. S., Kyle P. R. and Smellie J. S. (1997) Petrogenesis of a phonolite-trachyte succession at Mount Sidley, Marie Byrd Land, Antarctica. J. Petrol. 38, 1225–1253.
- Panter K. S., Blusztajn J., Hart S. R., Kyle P. R., Esser R. and McIntosh W. C. (2006) The origin of HIMU in the SW Pacific: Evidence from Intraplate Volcanism in Southern New Zealand and Subantarctic Islands. J. Petrol. 47, 1673–1704.
- Panter K. S., Castillo P., Krans S., Deering C., McIntosh W., Valley J. W., Kitajima K., Kyle P., Hart S. and Blusztajn J. (2018) Melt origin across a rifted continental margin: a case for subduction-related metasomatic agents in the lithospheric source of alkaline basalt, NW Ross Sea, Antarctica. *J. Petrol.* 59, 517–558.
- Perinelli C., Armienti P. and Dallai L. (2006) Geochemical and O-isotope constraints on the evolution of lithospheric mantle in the Ross Sea rift area (Antarctica). *Contrib. Mineral. Petrol.* 151, 245–266.
- Phillips E. H., Sims K. W. W., Blichert-Toft J., Aster R. C., Kyle P. R., Gaetani G. A., Wallace P. J. and Rasmussen D. J. (2018)
 The nature and evolution of mantle upwelling at Ross Island, Antarctica. *Earth Planet. Sci. Lett.* 498, 38–53.
- Rasmussen D. J., Kyle P. R., Wallace P. J., Sims K. W. W., Gaetani G. A. and Phillips E. H. (2017) Understanding degassing and transport of CO₂-rich alkalic magmas at Ross Island, Antarctica using olivine-hosted melt inclusions. *J. Petrol.* 58, 841–861.
- Reagan M. K., Volpe A. M. and Cashman K. V. (1992) U-238 Series Chronology of Phonolite Fractionation at Mount Erebus, Antarctica. Geochim. Cosmochim. Acta 56, 1401–1407.
- Rocchi S., Armienti P., D'Orazio M., Tonarini S., Wijbrans J. R. and Di Vincenzo G. (2002) Cenozoic magmatism in the western Ross Embayment: Role of mantle plume versus plate dynamics in the development of the West Antarctic Rift System. *J. Geophys. Res. Solid Earth* **107**, 2195.
- Rocchi S., Armienti P. and Di Vincenzo G. (2005) No plume, no rift magmatism in the West Antarctic Rift. In *Plates, Plumes,* and *Paradigms. Geol. Soc. Amer. Special Paper*, 388 (eds. G. R. Foulger, J. H. Natland, D. C. Presnall and D. L. Anderson), pp. 435–447.
- Ryerson F. J., Durham W. D. and Cherniak D. J. (1989) Oxygen diffusion in olivine-effect of oxygen fugacity and implications for creep. J. Geophys. Res. 94, 4105–4118.
- Sharp Z. D. (1990) A laser-based microanalytical method for the in-situ determination of oxygen isotope ratios of silicates and oxides. Geochim. Cosmochim. Acta 54, 1353–1357.
- Sims K. W. W., Blichert-Toft J., Kyle P. R., Pichat S., Bluzstajn J., Kelly P. J., Ball L. A. and Layne G. D. (2008) A Sr, Nd, Hf, and Pb isotope perspective on the genesis and long-term evolution of alkaline magmas from Erebus volcano, Antarctica. *J. Volcan. Geotherm. Res.* 177, 606–618.
- Sims K. W. W., Pichat S., Reagan M., Kyle P. R., Dunbar N., Gauthier P.-J., Blichert-Toft J., Sawyer G., Duvalia H., Prytulak J., Charrette M., Elliott T., Layne G., Ball L. and Andrews J. (2013) Determining the timescales of magma genesis, melt evolution, crystal growth rates and magma degassing in the Mt Erebus magmatic system from ²³⁸U–²³⁴U-²³⁰Th-²²⁶Ra-²¹⁰Pb-²¹⁰Po; ²³²Th-²²⁸Ra-²²⁸Th; and ²³⁵U-²³¹Pa-²²⁷Ac. *J. Petrol.* **54**, 235–271.
- Storey B. C., Leat P. T., Weaver S. D., Pankhurst R. J., Bradshaw J. D. and Kelly S. (1999) Mantle plumes and Antarctica-New

- Zealand rifting: evidence from mid-Cretaceous mafic dykes. *J. Geol. Soc. Lond.* **156**, 659–671.
- Taylor, Jr., H. P. (1979) Oxygen and hydrogen isotope relationships in hydrothermal mineral deposits. In *Geochemistry of Hydrothermal Ore Deposits* (ed. H. L. Barnes). J. Wiley and Sons, New York, pp. 236–277.
- Troch J., Ellis B. S., Harris C., Bachmann O. and Bindeman I. N. (2020) Low- δ^{18} O silicic magmas on Earth: A review. *Earth Sci. Rev.* **208** 103299.
- Wang Z., Kitchen N. E. and Eiler J. M. (2003) Oxygen isotope geochemistry of the second HSDP core. *Geochem. Geophys. Geosyst.* **4**, 1–29.
- Wang Z. and Eiler J. M. (2008) Insights into the origin of the low- δ^{18} O basaltic magmas in Hawaii revealed from in situ measurements of oxygen isotope compositions of olivines. *Earth Planet. Sci. Lett.* **269**, 377–387.

- Wardell L. J., Kyle P. R. and Chaffin C. (2004) Carbon dioxide and carbon monoxide emission rates from an alkaline intra-plate volcano: Mt. Erebus, Antarctica. J. Volcanol. Geotherm. Res. 131, 109–121.
- Woolf J., Grandy J. and Larson P. (2000) Interactions of mantlederived magma with island crust? Trace element and oxygen isotope data from the Diego Hernandez Formation, Las Canadas, Tenerife. J. Volcanol. Geotherm. Res. 103, 343–366.
- Zhao Z. F. and Zheng Y. F. (2003) Calculation of oxygen isotope fractionation in magmatic rocks. *Chem. Geol.* **193**, 59–80.
- Zindler A. and Hart S. (1986) Chemical geodynamics. *Annual Rev. Earth Planet. Sci.* **14.** 493–571.

Associate editor: Rosemary Hickey-Vargas